

1 **Stratifying IVF population endometria using a prognosis**
2 **gradient independent of endometrial timing**

3

4 Josefa Maria SANCHEZ-REYES, Ph.D.^{a,b,π}

5 Antonio PARRAGA-LEO, M.Sc.^{a,b,π}

6 Patricia SEBASTIAN-LEON, Ph.D.^a

7 Maria del Carmen VIDAL, M.D.^c

8 Diana MARTI-GARCIA, M.Sc.^{a,b}

9 Katharina SPATH, Ph.D.^d

10 Immaculada SANCHEZ-RIBAS, M.D., Ph.D.^e

11 Francisco José SANZ, Ph.D.^a

12 Nuria PELLICER, M.D., Ph.D.^c

13 Jose REMOHI, M.D., Ph.D.^{b,c}

14 Dagan WELLS, Ph.D.^{d,f}

15 Antonio PELLICER, M.D., Ph.D.^{b,g}

16 Patricia DIAZ-GIMENO, Ph.D.^{a*}

17

18 ^a IVIRMA Global Research Alliance, IVI Foundation, Instituto de Investigación

19 Sanitaria La Fe, Av. Fernando Abril Martorell 106, Torre A, Planta 1^a, 46026

20 Valencia, Spain.

21 ^b Department of Pediatrics, Obstetrics & Gynecology, University of Valencia, Av.
22 Blasco Ibañez 15, 46010 Valencia, Spain.

23 ^c IVIRMA Global Research Alliance, IVIRMA IVI Valencia, Plaza de la Policia
24 Local 3, 46015 Valencia, Spain.

25 ^d JUNO Genetics, Winchester house, Edmund Halley Rd. Science Park, Oxford
26 OX4 4GE, United Kingdom.

27 ^e IVIRMA Global Research Alliance, IVIRMA IVI Barcelona, Calle Mallorca 45,
28 08029 Barcelona, Spain.

29 ^f Nuffield Department of Women's & Reproductive Health, University of Oxford,
30 Level 3, Women's Centre John Radcliffe Hospital, Oxford OX3 9DU, United
31 Kingdom.

32 ^g IVIRMA Global Research Alliance, IVIRMA IVI Rome, Largo Ildebrando
33 Pizzetti 1, Piano Rialzato 00197 Rome, Italy.

34 ^π Josefa Maria SANCHEZ-REYES and Antonio PARRAGA-LEO are joint first
35 authors.

36

37 *Corresponding author:

38 **Patricia DIAZ-GIMENO**

39 IVIRMA Global Research Alliance, IVI Foundation, Instituto de Investigación
40 Sanitaria La Fe (IIS La Fe), Valencia, Spain.

41

42 Edificio Biopolo – Instituto de Investigación Sanitaria la Fe
43 Avenida Fernando Abril Martorell, 106 - Torre A, Planta 1ª, 46026 Valencia
44 Tel: +34 96 390 33 05
45 email: patricia.diaz@ivirma.com / patricia_diaz@iislafe.es

46

47 **Conflict of interest**

48 The authors report no conflicts of interest.

49

50 **Funding**

51 This study was supported by the IVI Foundation (1706-FIVI-048-PD); Instituto
52 de Salud Carlos III (ISCIII) and co-funded by the European Regional
53 Development Fund “A way to make Europe” (PI19/00537 [P.D.-G.]). Patricia
54 Diaz-Gimeno is supported by Instituto de Salud Carlos III (ISCIII) through the
55 Miguel Servet program (CP20/00118) co-funded by the European Union.
56 Patricia Sebastian-Leon is funded by Instituto de Salud Carlos III (ISCIII)
57 through the Sara Borrell postdoctoral program (CD21/00132 [P.S.-L.]) co-
58 financed by the European Union. Josefa Maria Sanchez-Reyes was supported
59 by a predoctoral fellowship program of the Generalitat Valenciana
60 (ACIF/2018/072 [J.M.S.-R.], BEFPI/2020/028 [J.M.S.-R.]). Antonio Parraga-Leo
61 (FPU18/01777 [A.P.-L.]) and Diana Marti-Garcia (FPU19/03247 [D.M.-G.]) were
62 supported by predoctoral fellowship programs of the Spanish Ministry of
63 Science, Innovation and Universities.

64

65 **Paper presentation information**

66 Some of the findings reported in this scientific article were presented at the 78th
67 American Society for Reproductive Medicine Scientific Congress & Expo
68 (ASRM) held in Anaheim, California, USA, October 22-26, 2022.

69 **ABSTRACT**

70 **Background:** Independent of endometrial timing, there are molecular causes of
71 implantation failure that disrupt the endometrial transcriptome in the mid-
72 secretory phase. However, the molecular mechanisms disrupting the window of
73 implantation (WOI) remain poorly understood. The molecular heterogeneity of
74 this endometrial disruption must be characterized to develop personalized and
75 more accurate diagnostic tools for preventive medicine, particularly for patients
76 with a high risk of endometrial failure.

77 **Objective(s):** This study aimed to stratify and characterize the disrupted WOI
78 patterns using endometrial timing-corrected whole gene expression and artificial
79 intelligence (AI) models in *in vitro* fertilization (IVF) patients undergoing
80 hormone replacement therapy (HRT).

81 **Study design:** This multicenter prospective study was conducted between
82 January 2019 and August 2022. Endometrial biopsies were collected during the
83 mid-secretory phase for whole endometrial transcriptome analysis using RNA-
84 Sequencing. To identify disruptions in the WOI, the transcriptomic variation due
85 to cyclic endometrial tissue changes was removed. Out of 195 biopsies
86 sequenced, 131 were derived from patients that met the clinical criteria to be
87 classified as having a poor prognosis (≥ 3 implantation failures, $n=32$) or good
88 prognosis (< 3 implantation failures, $n=99$). The 131 patients were randomly
89 allocated to training ($n=105$) and test ($n=26$) sets for biomarker signature
90 discovery and assessment of predictive performance, respectively. The
91 reproductive outcomes of the single embryo transfer immediately after biopsy
92 collection were analyzed. Differential gene expression and functional analyses
93 were performed to characterize molecular profiles. Finally, a quantitative

94 polymerase chain reaction (qPCR) assay was used to corroborate the
95 differential expression of six potential biomarkers.

96 **Results:** With the dichotomous clinical classification of poor or good
97 reproductive prognosis, there was no transcriptomic distinction between
98 patients with a history of implantation failures during HRT endometrial
99 preparation. Alternatively, using an AI model to stratify IVF patients based on
100 the probability of endometrial disruption revealed molecular and clinical
101 differences between profiles. Patients were stratified into four reproductive
102 prognosis-related profiles, p1 (n=24), p2 (n=14), c2 (n=32) and c1 (n=61). The
103 highest pregnancy rate (PR) was associated with c1 (91%) and the highest
104 ongoing pregnancy rate (OPR) was associated with c2 (78%), linking these
105 profiles to good reproductive prognoses. On the other hand, p1 had the highest
106 biochemical miscarriage rate (BMR; 43%) while p2 had the highest clinical
107 miscarriage rate (CMR; 43%). Notably, both p1 and p2 were related to lower PR
108 and OPR, supporting that these profiles were associated with poor prognoses.
109 Regarding the functional characterization in the poor prognosis profiles that
110 were linked to miscarriages, p1 was associated with an excessive immune
111 response against the embryo during early pregnancy stages, while p2 was
112 initially immune-tolerant but rejected the fetus in later stages due to the lack of
113 metabolic response.

114 **Conclusion(s):** This new AI-based prognostic stratification of IVF patients is
115 promising for the clinical management of endometrial-factor infertility in
116 precision medicine.

117 **Keywords:** gene expression signature, endometrial disruption, endometrial
118 function, artificial intelligence, transcriptomic stratification, infertility, precision
119 medicine.

120 INTRODUCTION

121 Maternal endometrial status is a key factor in successful embryo implantation
122 and development in assisted reproductive technologies (ARTs).¹ Cyclical
123 physiological changes occur in the endometrium during the luteal phase to
124 facilitate embryo implantation. Maximum uterine receptivity occurs during the
125 window of implantation (WOI) in the mid-secretory phase.²⁻⁵ To ensure
126 endometrial factor success, the endometrium must synchronize with the embryo
127 during the WOI,⁶⁻⁹ and endometrial function must be undisrupted.¹⁰⁻¹² After
128 successful embryo implantation, the endometrium must support placentation
129 and provide an optimal equilibrium of embryo-maternal interactions as well as
130 adequate vascularization for fetal growth.¹³

131 Despite the development of ARTs, approximately 35% of transferred euploid
132 embryos do not implant in anatomically normal uteri at the first attempt.¹⁴
133 Patients experiencing successive implantation failures are clinically classified as
134 having recurrent implantation failure (RIF), however, there is a lack of
135 consensus on the definition of RIF.^{14,15} The heterogeneous etiology and clinical
136 symptoms of RIF do not provide sufficient criteria to stratify patients.^{10,16} Indeed,
137 the molecular heterogeneity of RIF patients highlights opportunities to
138 characterize the molecular profiles that contribute to the interpatient variability,
139 discover new biomarkers and develop tailored treatments.

140 The combined use of transcriptomics and artificial intelligence (AI) algorithms
141 has significantly advanced the understanding of endometrial-factor infertility.^{10–}
142 ^{12,17–19} This work is laying the groundwork for new applications in precision
143 medicine and ARTs, facilitating the characterization of reproductive diseases,
144 patient diagnosis and prognosis. In this context, accurate patient stratification is
145 necessary to match treatment to the right patient.^{20–22}

146 Leveraging the use of AI algorithms, our group recently proposed a biomarker
147 signature in luteal-phase endometrial biopsies that stratifies ART patients
148 undergoing hormone replacement therapy (HRT) into poor or good reproductive
149 prognosis, independent of endometrial timing.¹² In contrast to previous studies
150 performed in natural cycles,¹⁰ this prospective study included clinical follow-up
151 to investigate if the prognostic transcriptome-based groups were related to
152 reproductive outcomes. Despite using a 404-gene panel, dichotomous patient
153 classification into poor or good prognosis was limited by the molecular
154 complexity of implantation failure that requires the identification of more
155 subtypes.¹²

156 Hence, the current prospective study was designed to use the whole
157 transcriptomic profile to reproduce and refine our previous classification in a
158 new cohort of patients undergoing HRT. Our new prognostic stratification
159 elucidates the molecular heterogeneity of the endometrial disruptions in the
160 mid-secretory phase, independent of endometrial timing.

161 **MATERIALS AND METHODS**

162 **Ethics statement**

163 This study was approved by the Ethics Committee of the Instituto Valenciano de
164 Infertilidad (Valencia, Spain; 1706-FIVI-048-PD). Written informed consent was
165 obtained from all participants.

166 **Participants and clinical follow-up**

167 Participants (n=291) were recruited for a multicentric, prospective study
168 between January 2019 and August 2022 at five private fertility clinics in Spain.
169 Participants were scheduled for endometrial evaluation before embryo transfer
170 due to medical indications, and met the following inclusion criteria: 18–50 years
171 old, with a body mass index (BMI) of 19–30 kg/m², undergoing HRT prior to
172 single embryo transfer (SET) with a good-quality embryo (euploidy guaranteed
173 by preimplantation genetic testing or oocytes from donors <35 years old), and
174 presenting an endometrial thickness >6.5 mm with trilaminar structure in
175 proliferative phase. Exclusion criteria were male-factor infertility (in cases with
176 autologous sperm) as the only treatment indication, untreated reproductive
177 pathologies that may compromise endometrial function, severe pre-menopausal
178 symptoms, uncontrolled systemic or metabolic disorders, and co-administered
179 medication that can interfere with ARTs.

180 Baseline participant characteristics were obtained from internal medical records,
181 in accordance with data protection laws in Spain.

182 **Study design**

183 IVF patients undergoing HRT were clinically classified according to their history
184 of implantation failures. Endometrial biopsies were collected during the mid-
185 secretory phase for RNA-Sequencing (RNA-Seq) analysis. An AI probabilistic
186 model was developed based on the transcriptome independent of endometrial

187 timing, avoiding biases in transcriptomic variation due to cyclical changes in the
188 endometrium (**Supplementary Material**). The AI-determined probability of a
189 poor prognosis was used to stratify the population. Finally, the clinical outcomes
190 and molecular functions of the stratified profiles were studied (**Figure 1**).

191 **Endometrial biopsy collection, sequencing and data processing**

192 Endometrial biopsies were obtained from the uterine fundus, using a cannula
193 (Pipelle Cornier, CCD Laboratories, Paris, France) under sterile conditions, after
194 approximately 120 hours of progesterone treatment in the HRT cycles.
195 Anonymized samples were stored in RNA-later® (Sigma-Aldrich, Madrid, Spain)
196 at -80°C. RNA was extracted using the miRNeasy Mini Kit following
197 manufacturer's instructions (Qiagen, Hilden, Germany). RNA quality was
198 assessed using the NanoDrop™ One (AF-00342, ThermoFisher Scientific,
199 Valencia, Spain) and 4200 TapeStation System® (Agilent, Valencia, Spain).
200 Only samples that met the following RNA quality criteria were included in the
201 study: 260/280 ratio ~2.0, 260/230 ratio=1.8–2.2, RNA integrity number (RIN)
202 ≥3 and RNA fragments with more than 200 nucleotides (DV200) ≥70%.

203 Samples were sequenced using the AmpliSeq for Illumina® Transcriptome
204 Human Gene Expression Panel²³ in a NextSeq 500/550 system. Raw data were
205 evaluated using FastQC²⁴. STAR²⁵ was employed to align high-quality data
206 using GRCh37/hg19 as a reference. Gene counts obtained using
207 featureCounts²⁶ were normalized using Voom transformation and quantile
208 normalization in limma.²⁷ Genes with low counts were filtered using EdgeR.²⁸
209 Outliers and possible batch effects detected using principal component analysis
210 (PCA) were corrected using limma linear models.²⁷ Finally, the transcriptomic
211 variation due to endometrial luteal phase timing effects was detected using a

212 transcriptomic endometrial dating (TED) model established by our group,¹⁹ then
213 removed using limma as we previously described.¹² Additional details about the
214 TED model are presented in **Supplementary Material**.

215 **Clinical classification of patients**

216 Patients were initially classified based on their clinical history of implantation
217 failures. Implantation failure was considered for patients who presented a
218 negative beta chorionic gonadotropin (β -hCG) value (≤ 10 IU/L) 14–16 days
219 following embryo transfer, or a biochemical miscarriage (defined by a positive
220 serum β -hCG value, but absence of pregnancy within the first 10 weeks of
221 gestation).¹⁴ Patients with at least three implantation failures were initially
222 classified as having an endometrium with a poor prognosis whereas patients
223 who achieved implantation success within the first three attempts, were initially
224 classified as having an endometrium with a good prognosis. Patients with
225 insufficient attempts were excluded from further analyses (n=62).

226 **Patient stratification based on AI algorithms**

227 A training set (80% of samples) was employed to identify a biomarker signature
228 for endometrial disruption in the mid-secretory phase, stratify patients and
229 develop an AI-based prediction model that was externally validated in an
230 independent testing set (20% of samples).

231 The training set was used for endometrial gene signature discovery, as
232 previously described.¹⁹ Briefly, genes were listed in decreasing order, based on
233 an informativity score, using CorrelationAttributeEval²⁹ in Weka.³⁰ To study the
234 predictive performance of different sets of ordered genes, five-fold cross-
235 validation processes with 100 iterations were performed independently with

236 support vector machine (SVM),³¹ k-nearest neighbors (kNN)³² and random
237 forest (RF) algorithms³³ using RWeka.³⁴ Among all the outputs, the signature
238 with the highest accuracy and most genes was selected and used to develop a
239 balanced probabilistic model (**Supplementary Material**). The probabilistic
240 model was internally evaluated through cross-validation (5-fold, 10 times) in 100
241 different balanced models and their performance was evaluated with the test
242 set. The range of poor prognosis probabilities obtained by running the AI model
243 in all samples was used to stratify the study cohort into the following good (c)
244 and poor (p) prognosis profiles: c1 (probability \leq 0.2), c2 (probability $>$ 0.2 &
245 probability $<$ 0.5), p2 (probability \geq 0.5 & probability $<$ 0.8), or p1 (probability \geq 0.8).

246 **Molecular characterization of the different transcriptomic profiles**

247 The differentially expressed genes (DEGs) [False Discovery Rate (FDR) $<$ 0.05]
248 between profiles were identified using limma. Next, the functional differences
249 between the profiles were revealed with gene set enrichment analyses (GSEA)
250 performed using ClusterProfiler³⁵. Biological functions were obtained from Kyoto
251 Encyclopedia of Genes and Genomes (KEGG; September 2021 version)³⁶ while
252 experimental annotated terms were obtained from Gene Ontology (GO;
253 December 2021 version).³⁷

254 **Remeasuring the expression of selected potential biomarkers**

255 The expression of six DEGs was evaluated in 20 samples (five samples per
256 transcriptomic profile) with quantitative polymerase chain reaction (qPCR) using
257 beta-actin (*ACTB*) as a housekeeping gene. RNA was reverse transcribed into
258 cDNA using the PrimeScript Reagent Kit (Perfect Real Time, Takara, Japan) on
259 a Thermocycler T3000 (Biometra, Ireland). The qPCR was carried out using

260 Power-Up SYBR Green (Thermo Fisher Scientific, MA, USA) on a StepOnePlus
261 System (Applied Biosystems, CA, USA). The specific primer sequences
262 (Invitrogen, Thermo Fisher Scientific, MA, USA) are presented in **Supplemental**
263 **Table 1**. Relative gene expression was calculated using the $\Delta\Delta\text{Ct}$ method³⁸ and
264 *ACTB* as a housekeeping gene.

265

266 **Statistical analysis**

267 Rates for reproductive outcomes [i.e., pregnancy (PR), cumulative pregnancy
268 (CPR), live birth (LBR), biochemical miscarriage (BMR) and clinical miscarriage
269 (CMR)] were calculated as described in the **Supplementary Material**.
270 Descriptive statistics were used to ensure homogeneity of the patients' baseline
271 clinical characteristics. Continuous variables were presented as an overall
272 mean \pm standard deviation, whereas discrete variables were presented as
273 counts and percentages. Statistical differences between groups were compared
274 using the Wilcoxon rank-sum test for continuous variables and the Fisher's
275 exact test for discrete variables. All statistical analyses were conducted in R
276 (version 4.0.5, 2021-03-31).³⁹ Graphical results were generated with ggplot2.⁴⁰
277 In all cases $p < 0.05$ was considered statistically significant.

278

279

RESULTS

280 **Transcriptomic data and clinical characterization of patients**

281 After quality control and analysis of available clinical information (see
282 **Supplementary Material** for details), 131 samples and 14,674 genes qualified

283 for evaluation. Patients were clinically classified as having an endometrium
284 associated with a poor (n=32) or good (n=99) prognosis based on the number
285 of previous implantation failures. Both groups were homogeneous in terms of
286 main clinical variables (e.g., number of patients, age, body mass index, infertility
287 type and duration, endometrial dating) (**Supplemental Table 2**), ensuring that
288 there were no potential biases in endometrial-factor transcriptomic differences.
289 As expected, the number of transfers and implantation failures were significantly
290 different between groups (p-value=2.20e-16) due to the clinical classification
291 criteria used for this study. However, pairwise comparison revealed there were
292 no significant differences between the good prognosis groups (c1 and c2).
293 Batch effects were corrected to ensure the transcriptomic differences were
294 related to endometrial disruption independent of endometrial timing (see
295 **Supplementary Material**).

296 **Four new prognostic stratification groups for endometrial function**

297 Participants were stratified into four profiles using a 236-gene signature and a
298 probabilistic model that predicts endometrial profiles with 77% accuracy, 67%
299 sensitivity and 80% specificity (see **Supplementary Material** for more details).
300 The four profiles were established as poor (p) or good (c) according to the
301 probability of presenting an endometrium associated with a poor prognosis: p1
302 (n=24) and p2 (n=14), c2 (n=32) and c1 (n=61). Clinical variables were
303 homogenous for all stratified profiles (**Table 1**).

304 As expected, the number of transfers and implantation failures were significantly
305 different between the four profiles. Profiles associated with a poor prognosis

306 showed lower PR (29.17%) and LBR (50.00%) coupled with higher CMR
307 (42.86%) and BMR (42.68%) compared to the good prognosis profiles (**Figure**
308 **2A**). These differences were statistically significant ($p\text{-value}\leq 0.05$) for all
309 outcomes except CMR (**Figure 2A**). Interestingly, the p1 profile was related to a
310 higher rate of biochemical miscarriages, the p2 profile was related to clinical
311 miscarriages and the c1 profile was associated with the best reproductive
312 outcomes. When groups were compared pairwise significant differences were
313 found between the p1 and c1 groups in terms of PR ($p\text{-value}=0.0011$), LBR ($p\text{-}$
314 $\text{value}=0.0478$) and BMR ($p\text{-value}=0.0018$); between p2 and c1 groups in terms
315 of LBR ($p\text{-value}=0.0147$) and CMR ($p\text{-value}=0.0478$), and finally, between the
316 p1 and c2 groups in terms of PR ($p\text{-value}=0.004$) (**Figure 2B**). Considering all
317 embryo transfer attempts, the cumulative PR reached 38% for p1, 76% for p2,
318 81% for c2, and 93% for c1 (**Figure 2C**).

319 **Molecular characterization of the transcriptomically-defined profiles**

320 With respect to c1, there were 47 DEGs identified in p2, 3 DEGs in p1 and 1
321 DEG in c2. Only one transcript, mitogen-activated protein kinase 8 interacting
322 protein 1 pseudogene (*LOC644172* or *MAPK8IP1P2*), was shared between p1
323 and c1 profiles, as well as c2 and c1 profiles (**Table 2**).

324 The p2 and p1 profiles showed the highest number of functional dysregulations
325 compared to c1 (54 and 38 dysregulations, respectively). The downregulated
326 functions (30/54, 55.6%) in p2 were mainly related to immune response ($n=10$)
327 or metabolism and energy production ($n=12$). The upregulated functions (24/54,
328 44.4%) in p2 were mainly related with nervous system and sensory perception

329 (n=6), gene expression and protein degradation (n=6). Compared to the c1
330 profile, the p1 profile had mainly upregulated functions (27/38, 71.1%), which
331 were related to immune responses (n=9), nervous system and sensory
332 perception (n=6). Notably, most of the downregulated functions (11/38, 28.9%)
333 in p1 were related to cellular movement and ciliary processes (n=6) (**Table 2**).

334 Both poor-prognosis-related profiles had a noticeable dysregulation of immune
335 responses compared to the c1 profiles. However, the p1 was characterized by
336 nine upregulated functions while the p2 was characterized by ten
337 downregulated functions. The p2 profile also presented 12 downregulated
338 functions related to metabolism and energy production (**Table 2**).

339 There were 22 functional dysregulations between the control profiles, with the
340 c2 presenting a dysregulated profile similar to p2. Specifically, the c2 profile
341 presented a downregulation of nine functions related to immune responses and
342 an upregulation of five functions related to the nervous system and sensory
343 perception (**Table 2**).

344 **Remeasuring expression of potential biomarkers of endometrial** 345 **disruption**

346 The expression of six DEGs was validated by qPCR. Three of these DEGs were
347 identified in the p1 vs. c1 comparison [DND microRNA-mediated repression
348 inhibitor 1 (*DND1*), synaptotagmin 10 (*SYT10*) and mitogen-activated protein
349 kinase 8 interacting protein 1 pseudogene (*LOC644172*)] or c2 vs. c1
350 comparison (*LOC644172*). The remaining three DEGs were selected for having
351 the highest absolute fold change between p2 and c1 [CF transmembrane

352 conductance regulator (*CFTR*), V-set domain containing T cell activation
353 inhibitor 1 (*VTCN1*) and solute carrier family 17 member 8 (*SLC17A8*]. Except
354 for *SLC17A8* (**Supplemental Figure 4**), all genes showed the same gene
355 expression trends in qPCR and RNA-Seq, reinforcing their role as potential
356 biomarkers of endometrial disruption.

357 **COMMENT**

358 **Principal findings**

359 This study is the first to stratify endometrial function into four transcriptomic
360 profiles, independent of endometrial timing. The four transcriptomic profiles
361 corresponded with significantly different reproductive rates, showing a gradient
362 of prognoses and highlighting the complex nature of endometrial disruption in
363 the mid-secretory phase.

364 **Results in the context of what is known**

365 Disrupted endometrial function, independent of luteal phase endometrial timing,
366 was associated with a heterogeneous transcriptomic behavior among IVF
367 patients undergoing HRT, as previously reported in patients undergoing natural
368 cycles.¹⁰ Our binary prediction model (good vs. poor prognosis) was based on a
369 signature of 236 genes that characterized the transcriptomic behavior with 67%
370 sensitivity. Our model's predictive performance exceeds that of Koot's binary
371 model, which was based on a larger signature of 301 genes and reached a
372 58.3% sensitivity when used to compare control and RIF patients in natural
373 cycles.¹⁰ Although we improved the predictive performance, these results

374 showed that using a dichotomous model to identify the gene expression
375 patterns associated with good or poor prognosis did not achieve sufficient
376 power. Our last study in patients undergoing HRT showed that stratifying
377 patients using a 404-gene panel instead of clinical criteria significantly
378 enhanced the transcriptomic and clinical differences between poor and good
379 prognosis profiles.¹² However, the probabilistic model was not tested in an
380 independent test set, impeding comparison of the model's performance. Thus,
381 in this study, the whole transcriptome was used to stratify patients into four
382 profiles according to an AI-computed probability of endometrial disruption.
383 Notably, the resulting gradient of prognoses distinguished two profiles that were
384 related to different types of miscarriages.

385

386 **Clinical and research implications**

387 This work characterized four new prognostic profiles that can be used to predict
388 reproductive outcomes in IVF patients with a history of implantation failures.
389 Specifically, the p1 transcriptomic profile was related to the worst prognosis,
390 characterized by the highest BMR and the lowest PR. On a molecular level, the
391 p1 was associated with an excessive immune response, suggesting that a poor
392 feto-maternal tolerance could be driving miscarriages in the early stages of
393 pregnancy.⁴¹ Moreover, the overall downregulation of ciliary processes in this
394 cohort of patients with RIF reinforces their role in uterine disorders.⁴²
395 Alternatively, the p2 profile was related to the highest CMR and a lack of
396 immune and metabolic responses. These findings suggest that implantation is
397 facilitated by an initial immune tolerance but miscarriage occurs in subsequent
398 pregnancy stages due to energetic deficiencies. This novel hypothesis about

399 the relevance of the endometrial factor in clinical miscarriages requires further
400 investigation. Finally, there were two good prognosis profiles characterized by
401 high PRs and LBRs. The c1 profile was related to the highest LBR and lowest
402 BMR.

403 Overall, this new taxonomy can help improve the precision of diagnosis and
404 treatment of infertile women. It lays the groundwork for a new generation of
405 tools for evaluating patients with suspected endometrial-factor infertility or
406 stratifying types of miscarriages. Additionally, the molecular and functional
407 differences between the reproductive prognosis profiles set the foundation for
408 the discovery of new biomarkers and/or tailored therapeutic targets for each
409 specific transcriptomic profile.

410 **Strengths and limitations**

411 This study proposed a novel stratification based on four whole-transcriptome-
412 based profiles with a gradient of reproductive prognosis for IVF patients
413 undergoing HRT, improving the results from the binary classification obtained in
414 our previous studies.¹² Additionally, this approach leverages AI-computed
415 probabilities which are more objective and robust than traditional approaches to
416 classify patients with endometrial-factor infertility based on the number of
417 implantation failures.

418 However, it is worth mentioning that due to the stratification into four groups and
419 the limited sample size by group, the AI model needs further optimization.
420 Further studies with larger patient cohorts are required to boost the statistical

421 power of the model for population inference, assess inter-cycle reproducibility,
422 and conduct rigorous prospective clinical trials prior to clinical implementation.⁴³

423

424

425 **Conclusions**

426 Regardless of endometrial timing, the heterogeneous endometrial function can
427 be leveraged to stratify IVF patients undergoing HRT. This study uncovers four
428 distinct prognostic groups reflecting disrupted molecular profiles related with the
429 highest BMR and CMR (p1 and p2, respectively) or less disrupted profiles
430 associated with the highest LBR (c1) and the highest PR (c2). These molecular
431 findings were linked to functional differences, highlighting overactive immune
432 responses in p1 and decreased metabolism in p2, and revealing potential
433 mechanisms of actions underlying the biochemical and clinical miscarriages in
434 this cohort. Taken together, our results support that good and poor endometrial
435 prognoses have evident molecular and clinical differences. These findings
436 advance the research in personalized diagnostic and therapeutic strategies in
437 reproductive medicine, particularly for patients with endometrial-factor infertility.

438

439 **Acknowledgements**

440 The authors thank the patients who participated in the study and the clinical
441 staff who contributed to their recruitment, especially Elena Labarta, Juan
442 Antonio García Velasco, Juan Giles, Ernesto Bosch, Agustín Ballesteros, Gema
443 Castellón, Marcos Ferrando, Graciela Kohls, Francesca Gelosi, Laura Caracena,

444 Marga Esbert, Isabel Llorens, Cristina Gaya, Mónica Toribio, and Fernando
445 Quintana. We would like to thank Ester Castillo and Lourdes Fernandez from
446 Illumina® Spain, for their technical support for sequencing. Finally, we
447 acknowledge Raquel Amigo and Cristina Cardona from the Biobank and
448 Genomics Unit of the IIS La Fe, respectively, for assisting biopsy storing and
449 processing.

450

451 REFERENCES

- 452 1. Strowitzki T, Germeyer A, Popovici R, Von Wolff M. The human
453 endometrium as a fertility-determining factor. *Human Reproduction Update*.
454 2006;12(5):617-630. doi:10.1093/humupd/dml033
- 455 2. Harper MJK. 10 The implantation window. *Baillière's Clinical Obstetrics and*
456 *Gynaecology*. 1992;6(2):351-371. doi:10.1016/S0950-3552(05)80092-6
- 457 3. Murphy CR. Uterine receptivity and the plasma membrane transformation.
458 *Cell Res*. 2004;14(4):259-267. doi:10.1038/sj.cr.7290227
- 459 4. Noyes RW, Hertig AT, Rock J. Dating the endometrial biopsy. *American*
460 *Journal of Obstetrics and Gynecology*. 1975;122(2):262-263.
461 doi:10.1016/S0002-9378(16)33500-1
- 462 5. Wilcox AJ, Baird DD, Weinberg CR. Time of Implantation of the Conceptus
463 and Loss of Pregnancy. *New England Journal of Medicine*.
464 1999;340(23):1796-1799. doi:10.1056/nejm199906103402304
- 465 6. Diaz-Gimeno P, Sebastian-Leon P, Sanchez-Reyes JM, et al. Identifying
466 and optimizing human endometrial gene expression signatures for
467 endometrial dating. *Human Reproduction*. 2022;37(2):284-296.
468 doi:10.1093/humrep/deab262
- 469 7. Díaz-Gimeno P, Ruiz-Alonso M, Sebastian-Leon P, et al. Window of
470 implantation transcriptomic stratification reveals different endometrial
471 subsignatures associated with live birth and biochemical pregnancy. *Fertility*
472 *and Sterility*. 2017;108(4):703-710. doi:10.1016/j.fertnstert.2017.07.007
- 473 8. Díaz-Gimeno P, Horcajadas JA, Martínez-Conejero JA, et al. A genomic
474 diagnostic tool for human endometrial receptivity based on the
475 transcriptomic signature. *Fertility and Sterility*. 2011;95(1).
476 doi:10.1016/j.fertnstert.2010.04.063

- 477 9. Díaz-Gimeno P, Ruiz-Alonso M, Blesa D, et al. The accuracy and
478 reproducibility of the endometrial receptivity array is superior to histology as
479 a diagnostic method for endometrial receptivity. *Fertil Steril*. 2013;99(2):508-
480 517. doi:10.1016/j.fertnstert.2012.09.046
- 481 10. Koot YEM, Van Hooff SR, Boomsma CM, et al. An endometrial gene
482 expression signature accurately predicts recurrent implantation failure after
483 IVF. *Sci Rep*. 2016;6(1):19411. doi:10.1038/srep19411
- 484 11. Sebastian-Leon P, Garrido N, Remohí J, Pellicer A, Diaz-Gimeno P.
485 Asynchronous and pathological windows of implantation: Two causes of
486 recurrent implantation failure. *Human Reproduction*. 2018;33(4):626-635.
487 doi:10.1093/humrep/dey023
- 488 12. Diaz-Gimeno P, Sebastian-Leon P, Spath K, et al. Predicting risk of
489 endometrial failure: a biomarker signature that identifies a novel disruption
490 independent of endometrial timing in patients undergoing hormonal
491 replacement cycles. *Fertility and Sterility*. Published online March
492 2024:S0015028224001900. doi:10.1016/j.fertnstert.2024.03.015
- 493 13. Duc-Goiran P, Mignot TM, Bourgeois C, Ferré F. Embryo–maternal
494 interactions at the implantation site: a delicate equilibrium. *European Journal
495 of Obstetrics & Gynecology and Reproductive Biology*. 1999;83(1):85-100.
496 doi:10.1016/S0301-2115(98)00310-8
- 497 14. Pirtea P, Cedars MI, Devine K, et al. Recurrent implantation failure: reality or
498 a statistical mirage?: Consensus statement from the July 1, 2022 Lugano
499 Workshop on recurrent implantation failure. *Fertility and Sterility*.
500 2023;120(1):45-59. doi:10.1016/J.FERTNSTERT.2023.02.014
- 501 15. Cimadomo D, Craciunas L, Vermeulen N, Vomstein K, Toth B. Definition,
502 diagnostic and therapeutic options in recurrent implantation failure: an
503 international survey of clinicians and embryologists. *Human Reproduction*.
504 2021;36(2):305-317. doi:10.1093/humrep/deaa317
- 505 16. Devesa-Peiro A, Sebastian-Leon P, Pellicer A, Diaz-Gimeno P. Guidelines
506 for biomarker discovery in endometrium: correcting for menstrual cycle bias
507 reveals new genes associated with uterine disorders. *Molecular human
508 reproduction*. 2021;27(4):gaab011. doi:10.1093/MOLEHR/GAAB011
- 509 17. Diaz-Gimeno P, Horcajadas JA, Martinez-Conejero JA, et al. A genomic
510 diagnostic tool for human endometrial receptivity based on the
511 transcriptomic signature. *Fertility and Sterility*. 2011;95(1):50-60.
512 doi:10.1016/j.fertnstert.2010.04.063
- 513 18. Diaz-Gimeno P, Ruiz-Alonso M, Sebastian-Leon P, Pellicer A, Valbuena D,
514 Simon C. Window of implantation transcriptomic stratification reveals
515 different endometrial subsignatures associated with live birth and
516 biochemical pregnancy. *Fertility and Sterility*. 2017;108(4):703-710.
517 doi:10.1016/j.fertnstert.2017.07.007

- 518 19. Diaz-Gimeno P, Sebastian-Leon P, Sanchez-Reyes JM, et al. Identifying
519 and optimizing human endometrial gene expression signatures for
520 endometrial dating. *Human Reproduction*. 2022;37(2):284-296.
521 doi:10.1093/humrep/deab262
- 522 20. Guttmacher AE, Collins FS. Genomic Medicine — A Primer. Guttmacher
523 AE, Collins FS, eds. *N Engl J Med*. 2002;347(19):1512-1520.
524 doi:10.1056/NEJMra012240
- 525 21. Mirnezami R, Nicholson J, Darzi A. Preparing for precision medicine. *N Engl*
526 *J Med*. 2012;366(6):489-491. doi:10.1056/NEJMp1114866
- 527 22. Bell J. Stratified medicines: towards better treatment for disease. *The*
528 *Lancet*. 2014;383:S3-S5. doi:10.1016/S0140-6736(14)60115-X
- 529 23. Illumina. AmpliSeq for Illumina Transcriptome Human Gene Expression
530 Panel. 2021. Accessed December 17, 2021.
531 [https://www.illumina.com/products/by-type/sequencing-kits/library-prep-](https://www.illumina.com/products/by-type/sequencing-kits/library-prep-kits/ampliseq-transcriptome-gene-expression-panel.html)
532 [kits/ampliseq-transcriptome-gene-expression-panel.html](https://www.illumina.com/products/by-type/sequencing-kits/library-prep-kits/ampliseq-transcriptome-gene-expression-panel.html)
- 533 24. Andrews S, Krueger F, Segonds-Pichon A, Biggins L, Krueger C, Wingett S.
534 FastQC: a quality control tool for high throughput sequence data. Published
535 online 2010. <http://www.bioinformatics.babraham.ac.uk/projects/fastqc>
- 536 25. Dobin A, Davis CA, Schlesinger F, et al. STAR: ultrafast universal RNA-seq
537 aligner. *Bioinformatics*. 2013;29(1):15-21. doi:10.1093/bioinformatics/bts635
- 538 26. Liao Y, Smyth GK, Shi W. featureCounts: an efficient general purpose
539 program for assigning sequence reads to genomic features. *Bioinformatics*.
540 2014;30(7):923-930. doi:10.1093/bioinformatics/btt656
- 541 27. Ritchie ME, Phipson B, Wu D, et al. Limma powers differential expression
542 analyses for RNA-sequencing and microarray studies. *Nucleic Acids*
543 *Research*. 2015;43(7):e47. doi:10.1093/nar/gkv007
- 544 28. Chen Y, Lun ATL, Smyth GK. From reads to genes to pathways: Differential
545 expression analysis of RNA-Seq experiments using Rsubread and the
546 edgeR quasi-likelihood pipeline. *F1000Research*. 2016;5.
547 doi:10.12688/F1000RESEARCH.8987.2
- 548 29. Witten IH, Frank E, Hall MA, Pal CJ. *Data Mining: Practical Machine*
549 *Learning Tools and Techniques*. Morgan Kaufmann; 2016.
550 doi:<https://doi.org/10.1016/C2015-0-02071-8>
- 551 30. Frank E, Hall M, Holmes G, et al. Weka-A Machine Learning Workbench for
552 Data Mining. In: *Data Mining and Knowledge Discovery Handbook*. Springer
553 US; 2009:1269-1277. doi:10.1007/978-0-387-09823-4_66
- 554 31. Noble WS. What is a support vector machine? *Nature Biotechnology*.
555 2006;24(12):1565-1567. doi:10.1038/nbt1206-1565

- 556 32. Zhang Z. Introduction to machine learning: K-nearest neighbors. *Annals of*
557 *Translational Medicine*. 2016;4(11). doi:10.21037/atm.2016.03.37
- 558 33. Breiman L. Random forests. *Machine Learning*. 2001;45(1):5-32.
559 doi:10.1023/A:1010933404324
- 560 34. Hornik K, Buchta C, Zeileis A. Open-source machine learning: R meets
561 Weka. *Comput Stat*. 2009;24(2):225-232. doi:10.1007/s00180-008-0119-7
- 562 35. Yu G, Wang LG, Han Y, He QY. ClusterProfiler: An R package for
563 comparing biological themes among gene clusters. *OMICS: A Journal of*
564 *Integrative Biology*. 2012;16(5):284-287. doi:10.1089/omi.2011.0118
- 565 36. Kanehisa M, Goto S. KEGG: Kyoto Encyclopedia of Genes and Genomes.
566 *Nucleic Acids Research*. 2000;28(1):27-30. doi:10.1093/nar/28.1.27
- 567 37. Ashburner M, Ball CA, Blake JA, et al. Gene ontology: Tool for the
568 unification of biology. *Nature Genetics*. 2000;25(1):25-29.
569 doi:10.1038/75556
- 570 38. Livak KJ, Schmittgen TD. Analysis of Relative Gene Expression Data Using
571 Real-Time Quantitative PCR and the 2- $\Delta\Delta$ CT Method. *Methods*.
572 2001;25(4):402-408. doi:10.1006/meth.2001.1262
- 573 39. R Core Team. *R: A Language and Environment for Statistical Computing*. R
574 Foundation for Statistical Computing; 2021. <https://www.R-project.org/>
- 575 40. Wickham H. *Ggplot2: Elegant Graphics for Data Analysis*. Springer-Verlag
576 New York; 2016. <https://ggplot2.tidyverse.org>
- 577 41. Sargent IL, Wilkins T, Redman CWG. Maternal immune responses to the
578 fetus in early pregnancy and recurrent miscarriage. *The Lancet*.
579 1988;2(8620):1099-1104. doi:10.1016/S0140-6736(88)90522-3
- 580 42. Devesa-Peiro A, Sebastian-Leon P, Garcia-Garcia F, et al. Uterine disorders
581 affecting female fertility: what are the molecular functions altered in
582 endometrium? *Fertility and Sterility*. 2020;113(6):1261-1274.
583 doi:10.1016/j.fertnstert.2020.01.025
- 584 43. Diaz-Gimeno P, Sebastian-Leon P, Pellicer A. Reply of the Authors: Altered
585 endometrial receptivity: walking across the long path of precision medicine.
586 *Fertility and Sterility*. 2024;122(3):551. doi:10.1016/j.fertnstert.2024.06.010

587

588

589

590 **TABLES**

591

592 **Table 1. Baseline characteristics and reproductive history of the stratified**

593 **groups.** Endometrial profiles (c1, c2, p2, and p1) are compared according to

594 the main clinical variables related to reproductive outcomes. Using the

595 transcriptomic endometrial dating (TED) model, endometria in early and late

596 secretory (ESE;LSE) classes were grouped as displaced (Ds) while early and

597 late mid-secretory (EMSE;LMSE) classes were grouped as on time (Ot). BMI,

598 body mass index; N/A, not available; No., number of.; P, primary; S, secondary.

599 ***p-value < 0.001; ^ap-value < 0.05 in p1 vs. c1; ^bp-value < 0.05 in p1 vs. c2; ^cp-

600 value < 0.05 in p2 vs. c1; ^dp-value < 0.05 in p2 vs. c2; ^ep-value < 0.05 in p2 vs.

601 p1.

602

| | c1 | c2 | p2 | p1 | p-value |
|-------------------------------------|---|--|---|--|-------------------------------|
| No. patients | 61 | 32 | 14 | 24 | N/A |
| Age (years) | 40.77 ± 4.41 | 39.84 ± 4.97 | 40.14 ± 4.44 | 42.5 ± 3.56 | 0.1686 |
| BMI (kg/m²) | 23.62 ± 3.97 | 22.53 ± 3.47 | 22.53 ± 3.34 | 22.22 ± 3.68 | 0.3324 |
| Infertility type | P = 48 (82.8%) S = 10 (17.2%) N/A = 3 | P = 23 (79.3%) S = 6 (20.7%) N/A = 3 | P = 12 (92.3%) S = 1 (7.7%) N/A = 1 | P = 18 (85.7%) S = 3 (14.3%) N/A = 3 | 0.8501 |
| Infertility duration (years) | 2.95 ± 2.86 | 3.31 ± 3.10 | 3.58 ± 1.87 | 2.8 ± 1.7 | 0.7943 |
| Endometrial dating (TED) | Ds = 41 (67.2%) Ot = 20 (32.8%) | Ds = 18 (56.3%) Ot = 14 (43.7%) | Ds = 7 (50.0%) Ot = 7 (50.0%) | Ds = 17 (70.8%) Ot = 7 (29.2%) | 0.4354 |
| No. embryo transfers | 1.75 ± 0.85 | 1.78 ± 0.91 | 2.71 ± 1.44 | 4.21 ± 1.32 | 5E-17 *** a, b, c, d, e |
| No. implantation failures | 0.75 ± 0.85 | 0.81 ± 1.00 | 2.00 ± 1.75 | 3.79 ± 1.14 | 4E-22 *** a, b, c, d, e |

603

604

605

606 **Table 2. Molecular regulation and functional differences between**
 607 **endometrial profiles.** The table shows the number of differentially expressed
 608 genes (DEGs) and the corresponding number of significantly up- or
 609 downregulated biological functions [False Discovery Rate (FDR) < 0.05],
 610 identified through a gene set enrichment analysis (GSEA), for each comparison.
 611 The number of biological functions in each functional groups is indicated
 612 between brackets.

| | p1 vs. c1 | | p1 vs. c2 | | p1 vs. p2 | | p2 vs. c1 | | p2 vs. c2 | | c2 vs. c1 | |
|--|-----------|------|-----------|------|-----------|------|-----------|------|-----------|------|-----------|------|
| DEGs | 3 | | 0 | | 0 | | 47 | | 0 | | 1 | |
| Functional Groups | UP | DOWN | UP | DOWN | UP | DOWN | UP | DOWN | UP | DOWN | UP | DOWN |
| Immune response (n=26) | 9 | 0 | 9 | 0 | 7 | 1 | 3 | 10 | 6 | 2 | 0 | 9 |
| Nervous system and sensory perception (n=6) | 6 | 0 | 1 | 1 | 1 | 1 | 6 | 0 | 2 | 0 | 5 | 0 |
| Signal transduction (n=7) | 3 | 2 | 2 | 2 | 0 | 0 | 2 | 0 | 0 | 0 | 1 | 0 |
| Metabolism and energy production (n=26) | 3 | 2 | 3 | 3 | 0 | 2 | 1 | 12 | 3 | 6 | 0 | 0 |
| Cellular movement and ciliary processes (n=8) | 2 | 6 | 0 | 0 | 0 | 0 | 0 | 3 | 0 | 2 | 0 | 1 |
| Cellular adhesion and membranes (n=11) | 1 | 0 | 0 | 0 | 3 | 2 | 3 | 3 | 3 | 2 | 3 | 0 |
| Gene expression and protein degradation (n=13) | 1 | 0 | 1 | 0 | 2 | 4 | 6 | 2 | 6 | 2 | 0 | 3 |
| Proliferation and differentiation (n=2) | 1 | 1 | 1 | 0 | 0 | 0 | 0 | 0 | 0 | 0 | 0 | 0 |
| Longevity and senescence (n=2) | 1 | 0 | 0 | 0 | 0 | 0 | 1 | 0 | 0 | 0 | 0 | 0 |
| Angiogenesis and coagulation (n=3) | 0 | 0 | 0 | 0 | 0 | 2 | 2 | 0 | 1 | 0 | 0 | 0 |
| TOTAL NUMBER OF DYSREGULATED FUNCTIONS | 27 | 11 | 17 | 6 | 13 | 12 | 24 | 30 | 21 | 14 | 9 | 13 |
| | 38 | | 23 | | 25 | | 54 | | 35 | | 22 | |

613

614

615

FIGURE CAPTIONS

616 **Figure 1. Study design.** *In vitro* fertilization (IVF) patients undergoing hormone
617 replacement therapy (HRT) were classified as having good or bad endometrial
618 prognosis profiles based on their reproductive histories. Endometrial biopsies
619 were processed for whole-transcriptome RNA-Sequencing. Following RNA-
620 Sequencing data normalization, the effect of endometrial luteal-phase timing
621 was corrected. Subsequently, an artificial intelligence model was developed to
622 stratify the population into four groups according to their probability of having a
623 poor prognosis. Transcriptomic evaluation and functional characterization were
624 followed by an analysis of clinical reproductive outcomes profiles are clinically
625 relevant.

626 **Figure 2. Clinical evaluation of transcriptomic profiles. (A)** Bar plot showing
627 the significant differences obtained through pairwise comparisons of different
628 profiles. PR, Pregnancy rate; LBR, Live birth rate; CMR, Clinical miscarriage
629 rate; BMR, Biochemical miscarriage rate. **(B)** Bar plot showing the cumulative
630 pregnancy rate from multiple embryo transfers. *p-value < 0.05; **p-value <
631 0.01; ***p-value < 0.001.

632

633

SUPPLEMENTARY MATERIAL

634 **Supplemental Table 1. Specific primers employed for qPCR**
635 **remeasurement of endometrial disruption biomarkers.**

636 *CFTR*, CF transmembrane conductance regulator; *DND1*, MicroRNA-mediated
637 repression inhibitor 1; FW, forward; *MAPK8IP1P2*, mitogen-activated protein

638 *kinase 8 interacting protein 1 pseudogene 2*, also known as *LOC644172*;
639 qPCR, quantitative polymerase chain reaction; RV, reverse; *SLC17A8*, solute
640 carrier family 17 member 8; *SYT10*, synaptotagmin; *VTCN1*, V-set domain
641 containing T cell activation inhibitor 1.

642 **Supplemental Table 2. Homogeneity of the baseline characteristics in**
643 **poor and good endometrial prognosis groups.**

644 With the transcriptomic endometrial dating (TED) model, early and late
645 secretory (ESE;LSE) classes were grouped as displaced while early and late
646 mid-secretory (EMSE;LMSE) classes were grouped as on time. BMI, body
647 mass index; N/A, not available; No., number of. ***p-value < 0.001.

648 **Supplemental Table 3. Homogeneity of the baseline characteristics in**
649 **training and test sets.** Baseline characteristics of training and test sets are
650 shown. With the transcriptomic endometrial dating (TED) model, early and late
651 secretory (ESE;LSE) classes were grouped as displaced while early and late
652 mid-secretory (EMSE;LMSE) classes were grouped as on time. BMI, body
653 mass index; N/A, not available; No., number of. *p-value < 0.05; ***p-value <
654 0.001.

655 **Supplemental Table 4. Comparison of AI model performance metrics.**

656 The table shows the performance metrics (accuracy, sensitivity, and specificity)
657 for individual machine learning models (SVM, RF, kNN) and their combinations
658 (SVM+kNN, SVM+RF, kNN+RF). kNN, k-Nearest neighbors; RF, Random
659 forest; SVM, Support vector machine.

660 **Supplemental Figure 1. Principal component analysis (PCA) results. (A)**

661 PCA plot identifying two outliers (V10 and Bi16), which were excluded from

662 subsequent analyses. **(B)** PCA plots depicting the batch effect from the
663 sequencing run before and after correction. **(C)** PCA plots depicting the
664 endometrial timing effect obtained using the 73-gene TED signature before and
665 after correction. EMSE, early mid-secretory; ESE, early secretory; LMSE, late
666 mid-secretory; LSE, late secretory; PC, principal component; TED,
667 transcriptomic endometrial dating.

668 **Supplemental Figure 2. Exploratory analysis of RNA quality parameters.**

669 Principal component analysis (PCA) plots for the **(A)** 260/230 ratio, **(B)** 260/280
670 ratio, **(C)** RNA fragments with more than 200 nucleotides (DV200), and **(D)** RNA
671 integrity number (RIN). No batch effects were observed for these parameters.

672 **Supplemental Figure 3. Selection of the poor endometrial prognosis gene**

673 **signature.** Graphs highlighting the maximum number of endometrial genes the
674 **(A)** Support vector machine (SVM), **(B)** k-Nearest neighbors (kNN) and **(C)**
675 Random Forest (RF) models can process with the highest accuracy. The
676 orange dotted line represents the percentage obtained with an unbalanced
677 proportion of good and poor prognosis classes.

678 **Supplemental Figure 4. qPCR validation of endometrial disruption**

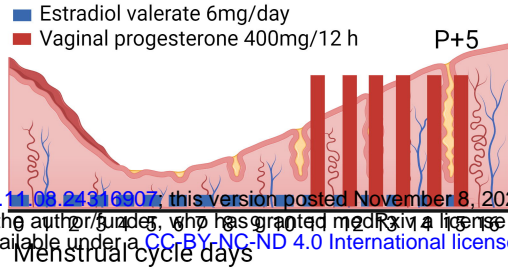
679 **biomarkers.** Comparison of gene expression fold change obtained with RNA-
680 Sequencing (RNA-Seq) and quantitative polymerase chain reaction (qPCR)
681 assays. Six differentially expressed genes (DEGS) were selected from **(A)** p1
682 vs. c1, **(B)** p2 vs. c1, **(C)** c2 vs. c1 comparisons.

683

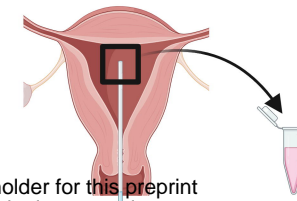
IVF population



Hormone replacement therapy (HRT)



Endometrial biopsy



Clinical variables

Clinical classification



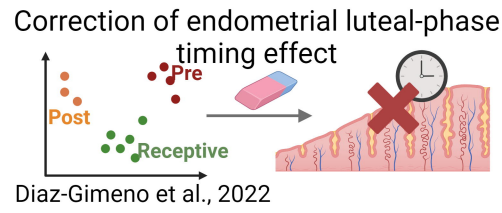
Poor prognosis



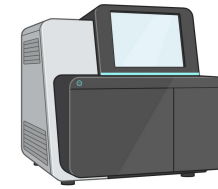
Unclassified



Good prognosis



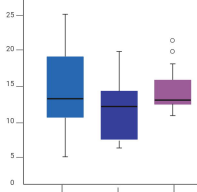
RNA-Sequencing



Excluded samples:
Low-quality or insufficient RNA
No clinical follow-up

AmpliSeq for Illumina® Transcriptome Human Gene Expression Panel

Performance evaluation

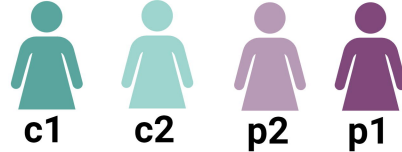
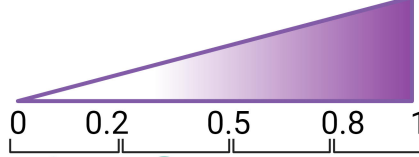


AI probabilistic models



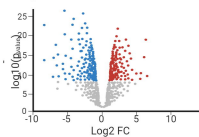
Population stratification

Poor prognosis probability

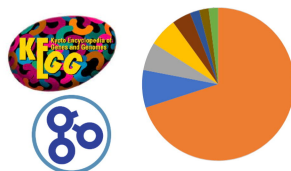


Molecular evaluation

Transcriptomic differences



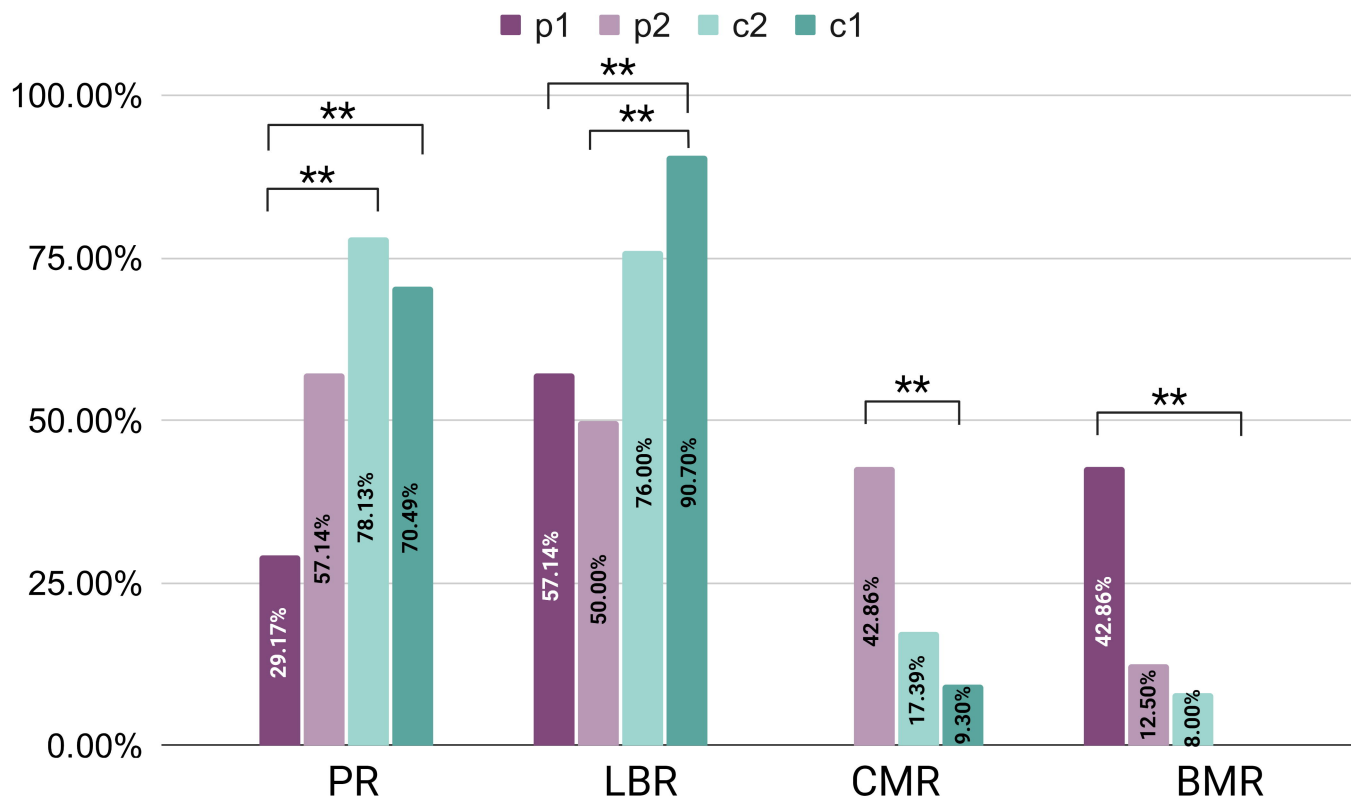
Functional characterization



Clinical evaluation



Reproductive rates

A)**B)**